PCCP

View Online
Dynamic Article Links

Cite this: DOI: 10.1039/c1cp22344e

www.rsc.org/pccp

PAPER

Solvation of hydrophobes in water and simple liquids

Kenichiro Koga*

Received 19th July 2011, Accepted 23rd August 2011
DOI: 10.1039/c1cp22344e

The solvation of nonpolar molecules in water and that in simple liquids are compared and contrasted. First, solvation thermodynamics is reviewed in a way that focuses on how the enthalpy and entropy of solvation depend on the choice of microscopic volume change v in the solvation process—including special choices v being zero (fixed-volume condition) and v being the partial molecular volume of a solute molecule (fixed-pressure condition)—and how the solvation quantities are related with temperature derivatives of the solvation free energy. Second, the solvation free energy and the solvation enthalpy of a Lennard-Jones (LJ) atom in model water are calculated in the parameter space representing the solute size and the strength of the solute–solvent interaction, and the results are compared with those for an LJ atom in the LJ solvent. The solvation diagrams showing domains of different types of solvation in the parameter space are obtained both for the constant-volume condition and for the constant-pressure condition. Similarities between water and the simple liquid are found when the constant-volume solvation is considered while a significant difference manifests itself in the fixed-pressure solvation. The domain of solvation of hydrophobic character in the parameter space is large in the constant-volume solvation both for water and for the simple liquid. When switched to the constant-pressure condition accompanying a microscopic volume change, the hydrophobic domain remains large in water but it becomes significantly small in the simple liquid. The contrasting results are due to the smallness of the thermal pressure coefficient of water at low temperatures.

1 Introduction

The solubility of nonpolar compounds in water is very low. A notable feature of the hydrophobicity is that the solubility decreases with increasing temperature at low temperatures—the hydrophobes become even more hydrophobic. The low solubility is a manifestation of an unfavorable solvation free energy and the decrease of solubility with increasing temperature is a manifestation of a favorable solvation enthalpy. To illustrate this point, the solvations of argon in water and in hydrazine are often compared.[1] The two solvents have striking similarity: they are hydrogen bonding liquids with nearly the same densities, dipole moments, and melting and boiling points. Solubilities of nonpolar atoms and molecules in hydrazine are very low as in water:[2] the solvation free energy μ^* of argon in water is 8.4 kJ mol^{-1}[3] and μ^* of argon in hydrazine is 9.9 kJ mol^{-1}.[4] However, the solvation enthalpy of argon in hydrazine is positive, *i.e.*, the solvation is energetically unfavorable and so it is not the one characteristic of the hydrophobic effect. On the other hand, there are some combinations of nonpolar solutes and nonpolar solvents in which the solvation is of hydrophobic character: the solvation free energy of argon in benzene is 3.5 kJ mol^{-1} and the solvation enthalpy is -14.3 kJ mol^{-1}.[3] Thus, benzene and water are the same kind of solvents but hydrazine is not, as regards the thermodynamic character of the solvation of argon.

It has long been recognized that the hydrophobic effect is important in chemistry and physics, in particular in understanding water,[5–7] and plays crucial roles in formation, stability, and functions of biological systems. There are thus a vast amount of studies, ranging from pioneering works[8–13] to recent extended accounts on the subject.[14–18] Computer simulations of realistic models of aqueous solutions provide detailed information on the hydrogen bonded network around solute molecules, the potential of mean force between solute molecules, and the effects of temperature and pressure on the hydrophobic hydration and interactions.[19,20] On the other hand, simple models are often useful for capturing some general features of hydrophobicity.[21–24]

Microscopic mechanisms of the negative solvation enthalpy of the hydrophobic hydration have been proposed in various forms. Several studies, however, have noted that thermodynamic properties of pure water such as the density maximum at 4 °C are the key to understand the hydrophobic hydration.[25] We will see in fact that the smallness of the coefficient of thermal

Department of Chemistry, Faculty of Science, Okayama University, 700-8530, Okayama, Japan. E-mail: koga@cc.okayama-u.ac.jp

expansion α_p, or of the thermal pressure coefficient γ_V, of water at low temperatures makes water significantly different from other solvents. In general (not restricted to particular solvents and solutes), the solvation thermodynamic quantities such as the solvation energy, enthalpy and entropy of a solute are strongly dependent on whether pressure p is fixed or volume V is fixed before and after transferring solute to solvent.[13,22,26–30] Even when the pV term is vanishingly small compared to the energy term, the difference between the solvation energy in the fixed-V process and the solvation enthalpy in the fixed-p process does *not* vanish and is typically 10 kT near the triple point of a solvent. If a fixed-volume condition is chosen, the solvation of Lennard-Jones (LJ) particles in the LJ solvent can be thermodynamically analogous to the hydrophobic hydration for wide ranges of the solute–solvent LJ size and energy parameters.[31] Here we examine variations of the solvation thermodynamic properties of LJ solutes in model water over the LJ size, energy parameter space. We calculate the variations both for the fixed-volume solvation and for the fixed-pressure solvation, and compare the general features for water with those for the LJ solvent.

In the following section, we review solvation thermodynamics with emphasis on the thermodynamic condition of solvation, either the volume is fixed, the pressure is fixed, or an arbitrary volume change is allowed. These conditions are in turn related to the solvation free energy change (or the solubility change) along isochoric, isothermal, and general paths in the temperature, pressure plane. In Section 3 we describe the model systems, the simulation method and conditions, and the calculation of solvation thermodynamic properties. Section 4 presents numerical results showing similarities and differences between water and the simple liquid as solvents of hydrophobes.

2 Review of solvation thermodynamics

Consider a homogeneous solution in which solute molecules of species A are present in a solvent. The solvation free energy μ^* of solute A in the system is defined as

$$\mu^* = -kT\ln(\rho_A/z_A) = \mu_A - \mu_A^{id}, \quad (1)$$

where ρ_A is the number density of solute molecules and z_A is the activity of solute A defined so as to become asymptotic to ρ_A in the limit that the total number density goes to zero. μ_A is the chemical potential of A in the system and μ_A^{id} is defined by the second equality and is referred to as an ideal part of μ_A. When solute A is a particle with the de Broglie thermal wavelength Λ, $z_A = (1/\Lambda^3)e^{\mu_A/kT}$ and $\mu_A^{id} = kT\ln(\rho_A\Lambda^3)$.

When the solution is in equilibrium with a dilute gas of solute A (phase α) with density ρ_A^α, the activity $z_A \simeq \rho_A^\alpha$ and so the solvation free energy μ^* is obtainable from the Ostwald adsorption coefficient ρ_A/ρ_A^α:

$$\mu^* = -kT\ln(\rho_A/\rho_A^\alpha). \quad (2)$$

If phase α is not a dilute gas, what one can measure from the partition coefficient is the difference in the solvation free energy of A between the solution of interest and phase α:

$$\Delta\mu^* = \mu^* - \mu^{*,\alpha} = -kT\ln(\rho_A/\rho_A^\alpha). \quad (3)$$

In molecular theoretical studies it is possible to examine μ^* in (1) without referring to another phase in equilibrium. In what follows we start from μ^* and consider its components, the solvation enthalpy and entropy, and their relations to temperature derivatives of μ^*. The thermodynamics for $\Delta\mu^*$ and its components and the relations to the temperature derivatives of the partition coefficient have been summarized earlier.[15]

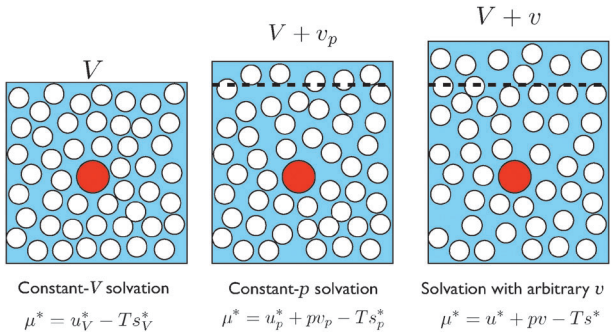

Fig. 1 Three thermodynamic conditions of a solvation process. Insertion of a molecule in the solvent with the volume V fixed (left), with the pressure p fixed and the volume changed by the partial molecular volume v_p (middle), and with the volume changed by an arbitrary microscopic volume v (right). The solvation free energy μ^* is independent of the choice of the thermodynamic condition. The solvation enthalpy and the solvation entropy depend upon the choice.

The definition of the solvation free energy μ^* in (1) has no reference to the thermodynamic condition of the solvation process, *i.e.*, whether the volume V is fixed, the pressure p is fixed, or neither V nor p is fixed, when a solute is inserted in the solvent. But whenever one wishes to decompose μ^* into an energetic contribution and an entropic one, one must specify the thermodynamic condition of the solvation process. Three thermodynamic conditions for a solvation process are shown schematically in Fig. 1. A microscopic volume change v_p in the constant-p solvation process (middle) and v in a general solvation process (right) are exaggerated in the figure. In reality, however, any microscopic volume change v for transferring a solute molecule into the solvent of a macroscopic volume V is neither discernible nor controllable.

2.1 Constant-V process

In the constant-V process, the number N_A of A molecules is increased or decreased by 1 while the numbers of molecules of all the substances other than A are fixed and T is fixed. Then μ_A and μ_A^{id} are decomposed as

$$\mu_A = u_V - Ts_V, \quad \mu_A^{id} = u_V^{id} - Ts_V^{id},$$

where

$$u_V = \left(\frac{\partial U}{\partial N_A}\right)_{V,T}, \quad s_V = \left(\frac{\partial S}{\partial N_A}\right)_{V,T} \quad (4)$$

and u_V^{id} and s_V^{id} are the corresponding partial derivatives of energy and of entropy of a hypothetical system consisting of non-interacting solute molecules with the same density ρ_A and the same temperature T. Then,

$$\mu^* = u_V^* - Ts_V^* \quad (5)$$

with

$$u_V^* = u_V - u_V^{id}, \quad s_V^* = s_V - s_V^{id}. \quad (6)$$

The solvation energy u_V^* is equivalent to the potential energy change due to insertion of a solute molecule A in the solution at fixed V. The solvation entropy s_V^* is equivalent to the configurational entropy change due to the insertion of A at a fixed position in the solution with V fixed.

2.2 Constant-p process

In the constant-p solvation process, the pressure is the same, the temperature is the same, and the volume changes by the partial molecular volume v_p before and after the insertion of a solute molecule A in the solvent. The chemical potential of A is the partial molecular Gibbs free energy: $\mu_A = u_p + pv_p - Ts_p$ with u_p the partial molecular energy and s_p the partial molecular entropy. From this and $\mu_A^{id} = u_V^{id} - Ts_V^{id}$, the solvation free energy is written as

$$\mu^* = u_p^* + pv_p - Ts_p^* = h_p^* - Ts_p^* \tag{7}$$

with

$$u_p^* = u_p - u_V^{id}, \quad s_p^* = s_p - s_V^{id}, \tag{8}$$

and

$$h_p^* = u_p^* + pv_p. \tag{9}$$

The solvation energy u_p^* is the potential energy change due to the insertion of A at fixed p. The solvation entropy s_p^* is equal to the configurational entropy change before and after the insertion of A at a fixed position at fixed p, *i.e.*, with the volume change v_p.

The difference in the solvation thermodynamic quantities between constant-p and constant-V processes is given by the identity[13,22,27–30]

$$h_p^* - u_V^* = T(s_p^* - s_V^*) = \frac{T\alpha_p}{\chi} v_p = T\gamma_V v_p, \tag{10}$$

where $\alpha_p = (1/V)(\partial V/\partial T)_p$ is the coefficient of thermal expansion and $\chi = (1/\rho)(\partial\rho/\partial p)_T$ the isothermal compressibility, and $\gamma_V = \alpha_p/\chi = (\partial P/\partial T)_V$ the thermal pressure coefficient.[32] The difference (10) is a product of the bulk solvent property $T\gamma_V$ and the only factor v_p reflecting the solvation of a molecule A in the solvent.

Any microscopic volume change v including $v = 0$ and $v = v_p$ in the solvation process has no consequences on the structure of the solvent molecules around the solute molecule. Nevertheless, the solvation energy difference $h_p^* - u_V^*$, or equivalently the solvation entropy difference $T(s_p^* - s_V^*)$, is not small in general and typically a few kT to 10 kT. This has been discussed earlier[13,26] and demonstrated for LJ solutions near the triple point.[31] The difference can be either positive or negative since γ_V and v_p can have either sign independently. In ordinary systems where $\gamma_V > 0$ and $v_p > 0$, one finds $h_p^* > u_V^*$ and $s_p^* > s_V^*$.

In the special circumstances, however, the difference vanishes:

$$h_p^* = u_V^* \text{ and } s_p^* = s_V^* \text{ if } \gamma_V = 0 \text{ or } v_p = 0. \tag{11}$$

The condition $\gamma_V = 0$ is realized for water and other liquids that exhibit density maxima ($\alpha_p = 0$) at T_{MD}, the temperature of maximum density. Thus for the hydrophobic hydration with $v_p > 0$,

$$\begin{aligned} s_p^* < s_V^* \quad &\text{if} \quad T < T_{MD} \\ s_p^* = s_V^* \quad &\text{if} \quad T = T_{MD} \\ s_p^* > s_V^* \quad &\text{if} \quad T > T_{MD}. \end{aligned} \tag{12}$$

Note that at the liquid–gas critical point of a solvent, $\alpha_p \to \infty$ and $\chi \to \infty$ but γ_V remains finite, and so the difference $s_p^* - s_V^*$ does not vanish.

2.3 Solvation process with an arbitrary volume change

We have seen that the constant-V and the constant-p conditions give different solvation enthalpies (u_V^* and h_p^*) and entropies (s_V^* and s_p^*) while μ^* is independent of the condition. In fact there are infinite ways to decompose μ^* into the enthalpic and entropic terms as we will see now. And the infinite ways are not just thought experiments but are related to infinite paths in the p, T plane along which the variation of μ^* is actually measured (see Section 2.4).

Consider a generalized solvation process in which the volume of the system changes by an *arbitrary microscopic amount* v while the temperature is the same before and after the insertion of a molecule A in the solvent (Fig. 1, right). The partial molecular energy, entropy, and volume in this process are

$$u = \left(\frac{\partial U}{\partial N_A}\right)_T, \quad s = \left(\frac{\partial S}{\partial N_A}\right)_T, \quad v = \left(\frac{\partial V}{\partial N_A}\right)_T, \tag{13}$$

where the differentiations are neither at fixed V nor at fixed p in general but are with $(\partial p/\partial V)_T$, a rate of increase of p with respect to the volume variation, fixed to a value consistent with the choice of v. From the general identity

$$\left(\frac{\partial X}{\partial N_A}\right)_T = \left(\frac{\partial X}{\partial N_A}\right)_{V,T} + \left(\frac{\partial X}{\partial V}\right)_T \left(\frac{\partial V}{\partial N_A}\right)_T \tag{14}$$

for the differentiation of thermodynamic quantities X as in (13) and the thermodynamic relations $(\partial S/\partial V)_T = T\alpha_p/\chi$ and $(\partial U/\partial V)_T = (T\alpha_p/\chi) - p$, one finds

$$u = u_V + \left(\frac{T\alpha_p}{\chi} - p\right)v, \quad s = s_V + \frac{\alpha_p}{\chi} v. \tag{15}$$

With these general partial molar quantities, u and s, consistent with a general volume change v, the chemical potential of solute A is written as

$$\mu_A = u + pv - Ts, \tag{16}$$

a generalization of $\mu_A = u_p + pv_p - Ts_p$. The solvation free energy is then given by

$$\mu^* = u^* + pv - Ts^* \tag{17}$$

with

$$u^* = u - u_V^{id}, \quad s^* = s - s_V^{id}. \tag{18}$$

The solvation energy u^* is the potential energy difference in the system before and after the insertion of a molecule A accompanying the microscopic volume change v, and the solvation

entropy s^* is equal to the configurational entropy difference in the system before and after the insertion of A at a fixed position accompanying the volume change v. The quantity $h^* = u^* + pv$ may be called a generalized solvation enthalpy. In the solvation process with the special choice $v = 0$, $h^* = h^*_V = u^*_V$. The difference in h^* between the solvation process accompanying an arbitrary volume change v and the one with V fixed ($v = 0$) is then

$$h^* - u^*_V = T(s^* - s^*_V) = \frac{T\alpha_p}{\chi} v = T\gamma_V v, \qquad (19)$$

a general relation which includes eqn (10) as a special case of $v = v_p$. The difference is not small in general, as remarked earlier.

2.4 Temperature dependence of the solvation free energy

We reviewed above that how μ^* is decomposed into the solvation enthalpy and entropy both for the constant-V process and for the constant-p process, or in general for the solvation process accompanying an arbitrary microscopic volume change v. We also noted that the difference $h^* - u^*_V = T(s^* - s^*_V)$ is not small and can be a few kT in general: h^* and u^*_V could be different in sign. Then a microscopic picture of the solvation inferred from u^*_p and s^*_p can be significantly different from the one inferred from u^*_V and s^*_V. But the structure of solvent molecules around the solute molecule in the system of volume $V + v$ is essentially the same as the one in the system of volume V, for V is macroscopic. Thus it is not beneficial to infer a microscopic picture of the solvation from the solvation enthalpy and entropy, although it is tempting to do so. What we can learn from decomposing μ^* into the solvation enthalpy and entropy is discussed below.

The solvation enthalpy and entropy are not directly measurable quantities at a given temperature; they are related with temperature derivatives of the solvation free energy μ^*, which is experimentally obtainable by eqn (2) when phase α is a dilute gas. From (4)–(6), the solvation energy and entropy for the constant-V process are

$$u^*_V = \left(\frac{\partial \mu^*/T}{\partial 1/T}\right)_V, \quad s^*_V = -\left(\frac{\partial \mu^*}{\partial T}\right)_V, \qquad (20)$$

where the temperature differentiations are at fixed volume of the system and fixed numbers of molecules of all the substances in the system. The analog of (20) for the constant-p process is from (4)–(6)

$$h^*_p = \left(\frac{\partial \mu^*/T}{\partial 1/T}\right)_p + kT^2\alpha_p, \quad s^*_p = -\left(\frac{\partial \mu^*}{\partial T}\right)_p + kT\alpha_p, \qquad (21)$$

where the temperature differentiations are at fixed pressure of the system and fixed numbers of molecules of all the substances in the system.

The temperature may be varied along any fixed line on the p, V, T surface when the numbers of molecules of all the substances are fixed. The rate of increase of μ^* with respect to the general temperature variation is

$$\left(\frac{\partial \mu^*}{\partial T}\right) = \left(\frac{\partial \mu^*}{\partial T}\right)_V + \left(\frac{\partial \mu^*}{\partial V}\right)_T \left(\frac{\partial V}{\partial T}\right), \qquad (22)$$

where the partial derivatives without any subscripts stand for those along any fixed line on the p, V, T surface. Let

$$\alpha = \frac{1}{V}\left(\frac{\partial V}{\partial T}\right), \qquad (23)$$

a coefficient of thermal expansion with the same understanding of the partial derivative. Note

$$\left(\frac{\partial \mu^*}{\partial V}\right)_T = \left(kT - \frac{v_p}{\chi}\right)\frac{1}{V} \qquad (24)$$

and

$$\left(\frac{\partial \mu^*}{\partial T}\right)_V = -s^* + \frac{\alpha_p}{\chi} v, \qquad (25)$$

an identity equivalent to the second equation of (19). From (22)–(25),

$$\left(\frac{\partial \mu^*}{\partial T}\right) = -s^* + kT\alpha + \frac{\alpha_p}{\chi} v - \frac{v_p}{\chi}\alpha, \qquad (26)$$

and from (17) and (26),

$$\left(\frac{\partial \mu^*/T}{\partial 1/T}\right) = u^* + pv - kT^2\alpha + (\alpha v_p - \alpha_p v)\frac{T}{\chi}. \qquad (27)$$

Eqn (26) relates a general temperature derivative of μ^* along a fixed line on the p, V, T surface specified by α and the solvation entropy in the general solvation process accompanying a volume change v. Likewise eqn (27) is the relation between a temperature derivative of μ^*/T and the solvation enthalpy $h^* = \mu^* + pv$. In general, the choice of the line on the p, v, T surface along which the temperature is varied is independent of the choice of v in the solvation process at fixed temperature: there is no unique way to relate α and v. But the fixed-volume solvation ($v = 0$) is related with the isochoric temperature variation ($\alpha = 0$) as in eqn (20), and the fixed-pressure solvation ($v = v_p$) is related with the isobaric temperature variation ($\alpha = \alpha_p$) as in eqn (21), simply because the relations are most natural. There is then a natural way to relate α and v. That is,

$$\alpha = \frac{\alpha_p}{v_p} v. \qquad (28)$$

With this choice of α, one finds

$$u^* + pv = \left(\frac{\partial \mu^*/T}{\partial 1/T}\right) + kT^2\alpha, \quad s^* = -\left(\frac{\partial \mu^*}{\partial T}\right) + kT\alpha. \qquad (29)$$

The rate of increase of p with respect to the temperature variation is

$$\left(\frac{\partial p}{\partial T}\right) = \frac{\alpha_p}{\chi v_p}(v_p - v). \qquad (30)$$

Eqn (29) is a general version of eqn (20) and (21): with $v = 0$ and $\alpha = 0$ it becomes eqn (20) and with $v = v_p$ and $\alpha = \alpha_p$ it becomes eqn (21).

The lines of the temperature variations projected on the p, T plane are shown in Fig. 2. The solvation energy u^*_V and entropy s^*_V in the constant-V process are given by the temperature dependence of μ^* in the fixed-V direction

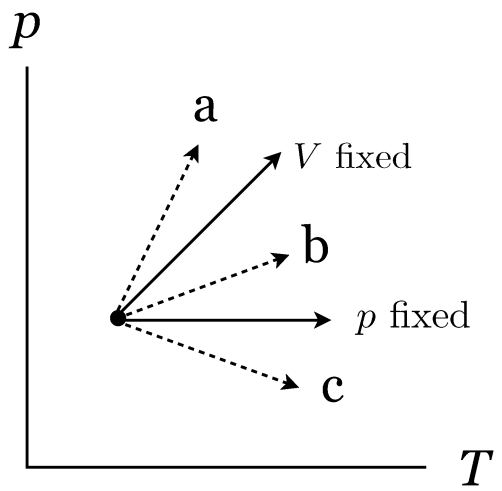

Fig. 2 Temperature variations projected on the p, T plane corresponding to different solvation processes. Here the coefficient of thermal expansion α_p and the partial molecular volume v_p are taken to be positive. V-fixed: isochoric temperature variation, $(\partial p/\partial T)_V = \alpha_p/\chi$, associated with the constant-V solvation process with u_V^* and s_V^* (Fig. 1, left). p-fixed: isobaric variation associated with the constant-p solvation process with h_p^* and s_p^* (Fig. 1, middle). a, b, c: temperature variations with slopes given by eqn (30), associated with the solvation process with an arbitrary volume change v (Fig. 1, left). a: $v < 0$; b: $0 < v < v_p$; c: $v > v_p$.

$(\partial p/\partial T)_V = \alpha_p/\chi$. Likewise, h_p^* and s_p^* are given by the variation of μ^* in the fixed-p direction. h^* and s^* in the solvation process accompanying an arbitrary volume change v are associated with the variation of μ^* in the direction with the slope given by (30). The temperature variations a, b, c in Fig. 2 illustrate those associated with the solvation processes

$$\begin{array}{llll} \text{a}: & v<0, & h^*<u_V^*, & s^*<s_V^*, \\ \text{b}: & 0<v<v_p, & u_V^*<h^*<h_p^*, & s_V^*<s^*<s_p^*, \\ \text{c}: & v_p<v, & h_p^*<h^*, & s_p^*<s^* \end{array}$$

in the case of $\alpha_p > 0$ and $v_p > 0$. In the special circumstance of $\alpha_p = 0$ as that of water at 4 °C, $h^* = u_V^*$ and $s^* = s_V^*$ for any microscopic volume change v, and correspondingly all the temperature variations associated with different choices of v become the isobaric variation $(\partial p/\partial T) = 0$. (All the arrows in Fig. 2 coincide with the one labeled "p fixed".)

The changes in various thermodynamic quantities accompanying the transfer of a molecule A from phase α to the phase of interest are given as the differences in solvation thermodynamic quantities between the phase of interest and phase α. From (5), (7), and (17),

$$\begin{aligned} \Delta\mu^* &= \Delta u_V - T\Delta s_V^* \\ &= \Delta h_p - T\Delta s_p^* = \Delta h - T\Delta s^*, \end{aligned} \tag{31}$$

superscripts "*" in u_V^*, h_p^*, and h^* being dropped because $\Delta u_V^* = \Delta u$, *etc.* The difference between the transfer with arbitrary volume changes and the fixed-V transfer is given as

$$\Delta h - \Delta u_V = T(\Delta s^* - \Delta s_V^*) = T\Delta\left(\frac{\alpha_p v}{\chi}\right). \tag{32}$$

3 Model systems and numerical methods

Two model solvents are examined: one is the TIP4P/2005 model of water[33] and the other is the LJ liquid. In both cases, a cubic simulation cell contains 500 solvent molecules under periodic boundary conditions. Then the solvation free energy of an LJ particle with varying size and energy parameters is obtained from molecular dynamics (MD) simulations or Monte Carlo (MC) simulations with the standard thermodynamic integration method.

For the water model, the temperature is set to 298.15 K and the mass density is fixed to be 1.00 g cm^{-3} with molar mass 18 g mol^{-1}. The corresponding dimension of the cubic cell is 24.63 Å. The original intermolecular potential function of the model water is tapered off in the range between 6.75 Å and 8.75 Å by a switching function. A nonpolar solute molecule is modeled by the LJ intermolecular interaction between the solute and TIP5P water molecules. The LJ size parameter σ for the solute–solvent interaction is taken to be 1.36, 2.04, 2.72, 3.44, 4.25, 5.1 Å. The dimensionless size parameter $\sigma^\bigstar = \sigma/\sigma_w$ ranges from 0.43 to 1.61, where $\sigma_w = 3.1589$ Å is the LJ size parameter of the model water molecule. The LJ energy parameter ε for the solute–solvent interaction is varied from 0 to 2.48 kJ mol^{-1}. The LJ parameter ε_w for the model water is 0.775 kJ mol^{-1}, and so the dimensionless energy parameter $\varepsilon^\bigstar = \varepsilon/\varepsilon_w$ ranges from 0 to 3.2.

Numerical calculation of μ^* as a function $\varepsilon^\bigstar$ for given $\sigma^\bigstar$ is efficiently done by the thermodynamic integration method.[34] The canonical-ensemble MD simulation is performed for the systems with the potential

$$\Psi(\lambda) = \Psi_0 + \lambda^n \Psi_A, \tag{33}$$

where Ψ_0 is the potential energy due to all the interactions among water molecules and Ψ_A the potential energy due to the interactions between a solute molecule A and all the water molecules; λ is a coupling parameter ranging from 0 to 1 and the power $n = 5$ is chosen here. The solvation free energy of a solute molecule A is then given by

$$\mu^* = n\int_0^1 \langle \lambda^{n-1}\Psi_A\rangle_\lambda \mathrm{d}\lambda, \tag{34}$$

where $\langle\cdots\rangle_\lambda$ denotes an average with the Boltzmann factor $\exp[-\Psi(\lambda)/kT]$. The integral is evaluated from twelve points in the range of λ with a common interval. The integrand in (34) at each λ is calculated from a set of independent MD simulations. The net simulation length for each λ ranges from 10 ns to 58 ns. The obtained data of the integrand in (34) are fit to a fifth degree polynomial. In all cases the fits are very well. The analytical integration of the polynomial gives μ^* as a function of $\varepsilon^\bigstar$ for each of the six different $\sigma^\bigstar$'s. The resulting μ^* is then interpolated with respect to $\sigma^\bigstar$ at fixed $\varepsilon^\bigstar$. The interval of $\varepsilon^\bigstar$ is taken to be 0.02 in the range from 0 to 2.40.

The solvation energy u_V^* in the constant-V process is directly obtained from the simulation at given λ as $\langle\Psi(\lambda)\rangle_\lambda - \langle\Psi_0\rangle_0$ with the same understanding of the average above and 0 denoting the system without a solute molecule. Then u_V^* is obtained as a function of $\sigma^\bigstar$ and $\varepsilon^\bigstar$.

The solvation enthalpy h_p^* in the constant-p process may be obtained directly from the isobaric–isothermal MD simulation; but the simulation length would be several times longer than the canonical simulation length in order to attain the same order of numerical accuracy for h_p^* as u_V^*. A more efficient way to evaluate h_p^* is to use the identity (10), $h_p^* - u_V^* = T\alpha_p v_p/\chi$, where u_V^* is obtained as described above. The coefficient of thermal expansion α_p is set to the experimental value 2.56×10^{-4} K^{-1} at 298 K; the TIP4P/2005 water model reproduces α_p very well,[33] so the value of the model water could have been used instead. The remaining factor is

$$\frac{v_p}{\chi} = \left[\rho\left(\frac{\partial\mu^*}{\partial\rho}\right)_T + kT\right]. \qquad (35)$$

The differential $(\partial\mu^*/\partial\rho)_T$ is evaluated as $\Delta\mu^*/\Delta\rho$, where $\Delta\rho$ is taken to be 0.05 g cm^{-3} and μ^* at 1.05 g cm^{-3} is obtained by repeating the same procedure as μ^* at 1.00 g cm^{-3} is obtained. We confirmed μ^* being essentially linear with respect to ρ in this range.

For the LJ solvent–LJ solute systems, we used the data generated from the MC simulations in our earlier study. In the canonical ensemble MC simulations, the temperature and the density are set to those close to the triple point of the LJ solvent: $T^\star = 0.7$, $\rho^\star = 0.8507$. In the isothermal–isobaric MC simulations, the corresponding pressure $p^\star = 0.12$ is chosen at the same temperature. Details of the simulations and the thermodynamic integration method are given in the previous report.[31]

4 Similarities and differences between water and a simple liquid as solvents

Variations of the solvation free energy in the solute–solvent interaction parameter space give some general trends in the solvation of a simple solute in the two solvents. Fig. 3 shows contours of constant μ^*/kT in the $\sigma^\star$, $\varepsilon^\star$ plane: (a) those for the LJ solvent and (b) those for the model water. The results are obtained from the NVT ensemble MC and MD simulations, but the same contour plots should be given from the NPT ensemble simulations[35] since μ^* is independent of the types of solvation processes illustrated in Fig. 1. Qualitative similarities in variation of μ^* between the simple liquid and water are apparent: (i) μ^* is positive and large (5 kT or larger) in the parameter region with large $\sigma^\star$ and small $\varepsilon^\star$, *i.e.*, a large solute molecule with a small attractive interaction with solvent molecules is practically insoluble; (ii) μ^* rises with decreasing $\varepsilon^\star$ (except at unphysically small $\varepsilon^\star$) and the slope is steeper at large $\sigma^\star$; (iii) μ^* increases with increasing $\sigma^\star$ at small $\varepsilon^\star$, but it does not at large $\varepsilon^\star$; and (iv) the contour of $\mu^* = 0$ (thick curves in the figure) extends from a point of small $\sigma^\star$ and small $\varepsilon^\star$ to a point of large $\sigma^\star$ and large $\varepsilon^\star$. There are quantitative differences in contours of μ^*/kT between the two solvents. The $\varepsilon^\star$ for the LJ solvent is the ratio of strength of the solute–solvent attraction to the solvent–solvent one. However, $\varepsilon^\star$ for the solvent of model water is a measure of the ratio of the solute–solvent ε to ε_w a *part* of the cohesive energy between water molecules. If $\varepsilon^\star$ for water were defined as a ratio of the solute–solvent pair cohesive energy ε to a measure of the *net* pair cohesive energy including the hydrogen-bond interaction, then the quantitative differences between the two systems would be less with respect to the scale of $\varepsilon^\star$.

Now general features of the solvation energy u_V^* in the constant-V process are compared for the two solvent models. Variations of u_V^* with varying σ and ε of the solute–solvent LJ potential are plotted as contours of constant u_V^*/kT in Fig. 4. Several common features are found between the simple liquid and water. A notable one is that u_V^* is negative over a major part of the parameter space; it is positive only when $\varepsilon^\star$ is much smaller than 1. This suggests that the solvation of inert gases or hydrocarbons in the constant-V process is energetically favorable in general, whether the solvent is a simple liquid or water. Since that would be also true for the solvation of polar solutes, it is reasonable to say that near the triple point of a solvent, the constant-V solvation of a solute molecule, whether it is polar or nonpolar, is almost always energetically favorable. Another common feature is that the solvation energy u_V^* rapidly decreases as both $\sigma^\star$ and $\varepsilon^\star$ increase.

Fig. 5 shows variations of the solvation enthalpy h_p^* in the constant-p process on the $\sigma^\star$, $\varepsilon^\star$ plane. The contour plot of h_p^*/kT for the LJ solvent (Fig. 5a) is significantly different from the corresponding plot of u_V^*/kT (Fig. 4a); it is rather similar

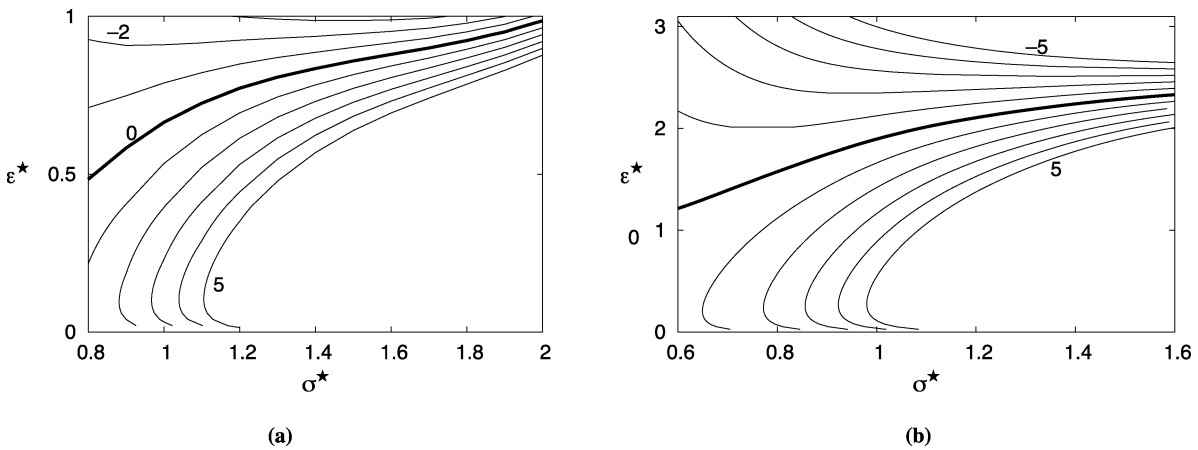

Fig. 3 Contours of constant μ^*/kT of a Lennard-Jones (LJ) solute (a) in the LJ solvent and (b) in the model water. $\sigma^\star$ and $\varepsilon^\star$ are the ratio of the solute–solvent LJ parameters to those of the solvent–solvent LJ interaction.

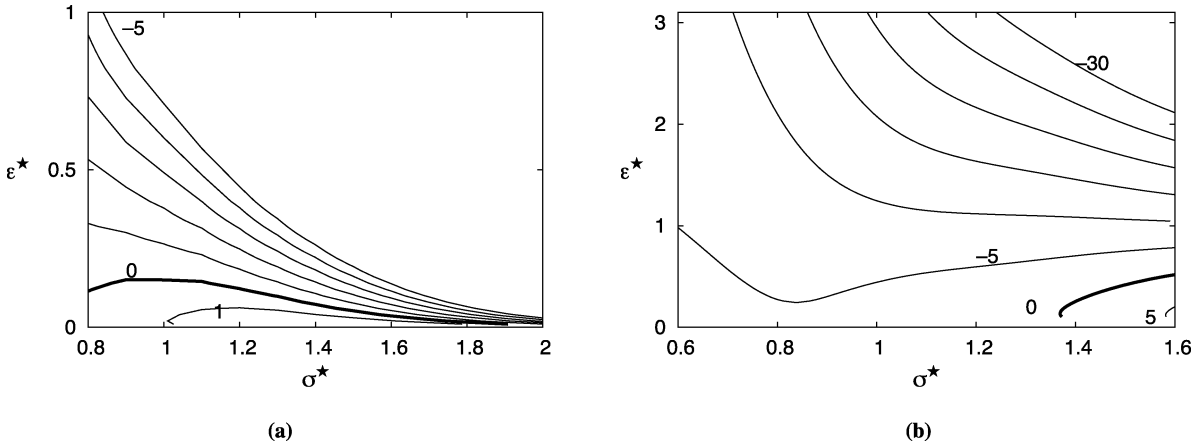

Fig. 4 Contours of constant u_V^*/kT of the LJ solute (a) in the LJ solvent and (b) in the model water.

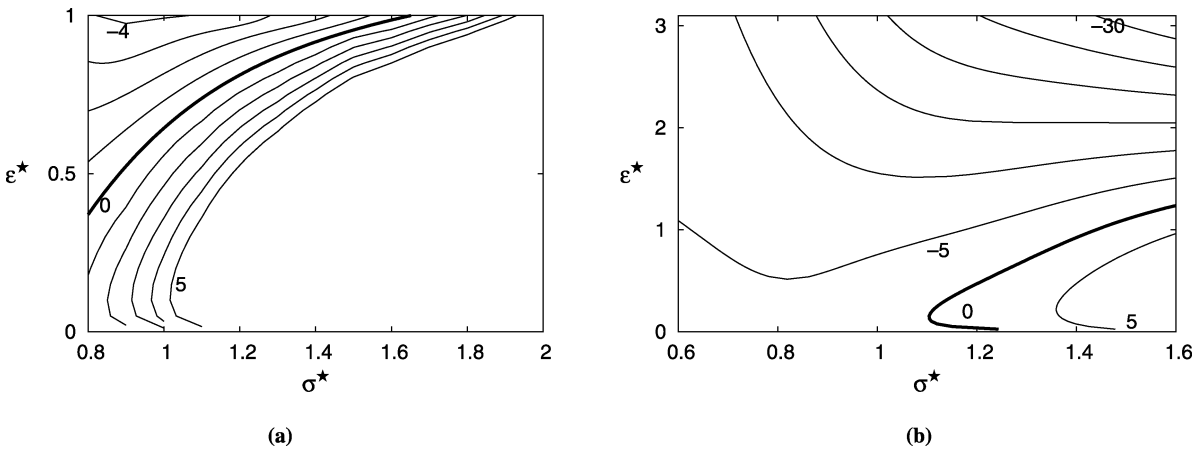

Fig. 5 Contours of constant h_p^*/kT of the LJ solute (a) in the LJ solvent and (b) in model water.

to μ^*/kT (Fig. 3a). The contour of $h_p^* = 0$ extends from a point of small $\sigma^\star$ and small $\varepsilon^\star$ to a point of large $\sigma^\star$ and large $\varepsilon^\star$. The h_p^* is positive and large at large $\sigma^\star$ and small $\varepsilon^\star$ and negative at small $\sigma^\star$ and large $\varepsilon^\star$. On the other hand, the contour plot of h_p^*/kT for the model water (Fig. 5b) is *not* very different from the plot of u_V^*/kT (Fig. 4b), that is, difference $(h_p^* - u_V^*)/kT$ is small in the $\sigma^\star$, $\varepsilon^\star$ parameter space. This is because α_p of water at 25 °C is much smaller than those of other liquids near their triple points. As remarked earlier the difference vanishes when $\alpha_p = 0$ at 4 °C. That $(h_p^* - u_V^*)/kT = \alpha_p v_p/k\chi$ is much smaller in water than in simple liquids is a notable feature of the hydrophobic hydration that comes from the thermodynamic property of pure water.

Fig. 6 shows constant-volume solvation diagrams in the $\sigma^\star$, $\varepsilon^\star$ plane for the LJ solvent and for the model water. The diagrams indicate the domains of three distinct types of the solvation: (i) $\mu^* > 0$ and $u_V^* < 0$; (ii) $\mu^* > 0$ and $u_V^* < 0$; and (iii) $\mu^* < 0$ and $u_V^* < 0$. The solvation of the second type is characteristic of the hydrophobic hydration: the solubility is low ($\mu^* > 0$) and the solvation is exothermic ($u_V^* < 0$), or in other words the solubility decreases with increasing temperature along an isochore or "V fixed" path as illustrated in Fig. 2. Both for the LJ solvent (Fig. 6a) and the model water (Fig. 6b), the domain of $\mu^* > 0$ and $u_V^* < 0$ is large in the parameter space, indicating that in the constant-V process, the solvation of hydrophobic character is not limited to hydrophobes in water but is found for nonpolar solutes in various solvents. Overall the solvation diagrams for the simple solvent and for water are qualitatively similar to each other.

Shown in Fig. 7 are the constant-pressure solvation diagrams for the LJ solvent and for water. The two diagrams are qualitatively different. In the diagram of the LJ solvent (Fig. 7a), the solvation of hydrophobic character ($\mu^* > 0$ and $h_p^* < 0$) is realized in a narrow region in the parameter space. In the case of water (Fig. 7b), however, the domain of hydrophobic hydration occupies a large portion of the parameter space. Another way of looking at the contrasting features is that when the solvation process in the LJ solvent is changed from the fixed volume to the fixed pressure condition, the domain of exothermic solvation ($h^* < 0$) in the $\sigma^\star$, $\varepsilon^\star$ space changes significantly, as has been seen as the notable difference between Fig. 4a and 5a. And it changes in such a way that the "hydrophobic" region ($\mu^* > 0$ and $h^* < 0$) shrinks significantly. This has been found in our earlier study.[31] In the case of water, the difference $h_p^* - u_V^*$ is small due to the small value of α_p, and so the "hydrophobic" region ($\mu^* > 0$ and $h^* < 0$) does not shrink very much and remains large when the solvation process is changed from the fixed-V to the fixed-p condition: see the notable similarity between Fig. 6b and 7b.

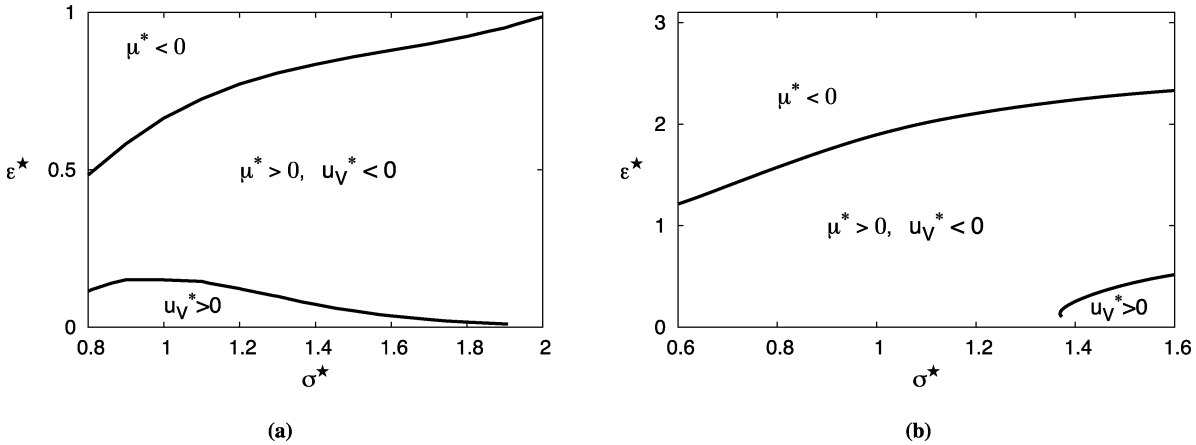

Fig. 6 Solvation diagram for the constant-volume solvation process (a) in the LJ solvent and (b) in model water. In each diagram there are two thick curves, one representing points of $u_V^* = 0$ and the other being those of $\mu^* = 0$.

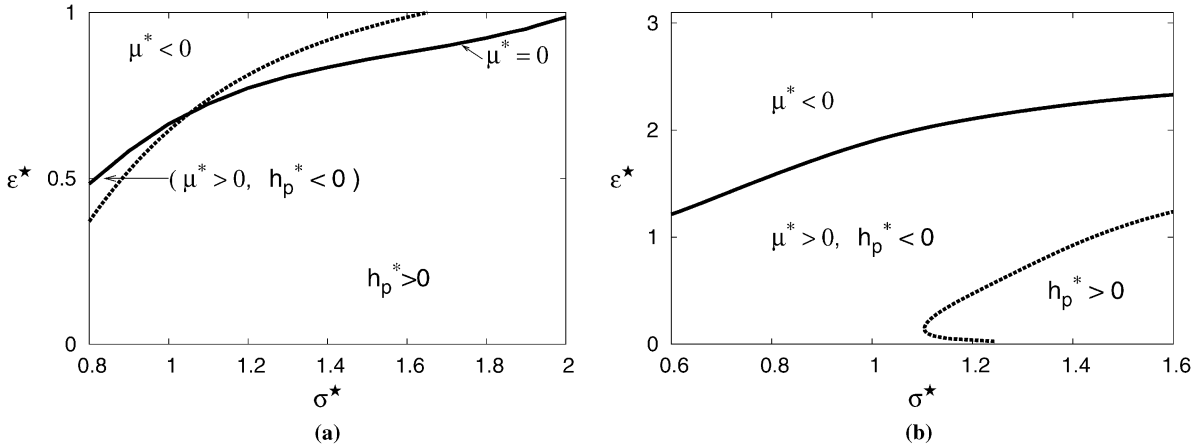

Fig. 7 Solvation diagram for the constant-pressure solvation process (a) in the LJ solvent and (b) in model water. In each diagram the dotted curve is the manifold of $h_p^* = 0$ and the solid curve is of $\mu^* = 0$.

In Section 2.3, we discussed the general solvation process accompanying an arbitrary microscopic volume change v. Now consider how the solvation diagram would be if v is chosen to be cv_p, where c is a constant factor. The $c = 1$ corresponds to the diagrams in Fig. 7. If the factor c is sufficiently larger than 1, the domain of hydrophobic character ($\mu^* > 0$ and $h^* < 0$) in the LJ solvent would disappear because the manifold of $h^* = 0$ shifts up and left in the diagram of Fig. 7a. The large domain of hydrophobic hydration of water at 298.15 K shown in Fig. 7b also becomes smaller if c is larger than 1 and would disappear if c is sufficiently large. At 4 °C where $\gamma_V = 0$, however, the solvation diagram of water would be independent of different choices of v or c because $h^* = u_V^*$ for all v. It is to be reminded that the solvation diagrams with different choices of v are not just results of the thought experiment. The general solvation process with $v = cv_p$ is related to a temperature variation with $\alpha = c\alpha_p$ in the p, T plane [see eqn (28)], and so, the solvation diagram for the process with the volume change $v = cv_p$ tells us the temperature dependence of μ^* and the solubility of the solute molecule when the temperature is varied as $\alpha = c\alpha_p$ in the p, T plane.

5 Summary and discussion

We studied similarities and differences in solvation between nonpolar solutes in water and in simple liquids, examining the solvations under fixed-volume and fixed-pressure conditions. It is worth emphasizing here that the difference between the solvation energy in the fixed-V process and the solvation enthalpy in the fixed-p process is not small and typically 10 kT near the triple point of a solvent; it does not, however, mean that microscopic structure of solvent molecules around a solute molecule is different. As given in eqn (10), the difference comes from a bulk property of the pure solvent and the partial molar volume of the solute.[13,22,27–30]

In the review of the solvation thermodynamics (Section 2), it was noted that the solvation process accompanying an arbitrary microscopic volume change v may be defined (Fig. 1, right). The solvation free energy μ^*, which is independent of the choice of v, is in general expressed as $u^* + pv - Ts^*$ as in eqn (17), where the solvation energy u^* (or enthalpy $h^* \equiv u^* + pv$) and the solvation entropy s^* depend on v. The constant-V solvation, a condition often assumed in molecular theories of solvation, is a special case $v = 0$; the constant-p solvation,

Table 1 Thermodynamic properties of liquids at the triple point.[32] Additional data of water at higher temperatures are those along the saturation curve

	$10^3\alpha_p/K^{-1}$	$10^4\chi/bar^{-1}$	γ_V/bar K^{-1}
Argon	4.39	2.04	21.6
Methane	2.93	1.47	19.9
Benzene	1.20	0.828	14.5
Water	−0.069	0.509	−1.35
Water at 20 °C	0.207	0.459	4.51
Water at 80 °C	0.641	0.461	13.9

which is the standard condition in experiment, corresponds to the choice $v = v_p$. The difference $h^* - u_V^*$ between the solvation enthalpy with an arbitrary volume change v and the one with $v = 0$ is equal to $T\gamma_V v$ as given by (19), which includes the identity (10) for the case $v = v_p$. It was also remarked that there is no unique way to relate the solvation process with an arbitrary volume change v and the temperature variation in the p, V, T surface. But if a particular choice (28) is made, the solvation enthalpy h^* and entropy s^* are related with the temperature derivatives of μ^* by eqn (29), which is a natural generalization of (20) and (21).

The thermal pressure coefficient γ_V is a thermodynamic property of the solvent. When $\gamma_V = 0$, the solvation enthalpy h^* and the solvation entropy s^* become independent of the choice of v, thereby being identical to u_V^* and s_V^*, respectively. Table 1 shows experimental data of the coefficient α_p of thermal expansion, the isothermal compressibility χ, and γ_V for nonpolar solvents and water. The values of α_p for water at and near the triple point are much smaller than those of argon, methane and benzene at the triple point, and $\gamma_V = \alpha_p/\chi$, too, is much smaller in water than in the nonpolar solvents. The smallness of γ_V in water is a key to understand why the solvation diagram of water for the constant-p process is significantly different from that of the simple liquid.

There are common features between the simple liquid and water as solvents of nonpolar solutes. First, as shown in Fig. 3a and b, general trends in variation of μ^* as functions of the solute–solvent interaction parameters $\sigma^\star$, $\varepsilon^\star$ are similar between the LJ solvent and water. Second, the variations of u_V^* in the parameter space for the two solvents are qualitatively similar to each other (Fig. 4). And third, when the constant-volume condition is assumed, there is a large region in the parameter space in which the solvation is of hydrophobic character (Fig. 6).

However, for ordinary liquids with γ_V typically in a range 15–20 bar K^{-1}, the constant-pressure solvation diagram is significantly different from the constant-volume solvation diagram: the domain of hydrophobic character in the constant-p solvation is considerably smaller than that in the constant-V solvation. As noted earlier[31] this is consistent with the experimental observation that the solvation of hydrophobic character is indeed found for nonpolar solvents but only when the solute is much smaller than solvent molecules. On the other hand, γ_V of water is one order smaller than those of ordinary liquids near the triple point. Consequently, the solvation diagram of water at low temperatures is nearly independent of whether V or p is fixed in the solvation process, and so the domain in parameter space in which the solvation is of hydrophobic character remains large in the constant-pressure solvation process. The notable difference between the simple liquid and water manifests itself in how the solvation diagram changes when the thermodynamic condition is changed from the one at fixed volume to the one at fixed pressure, as illustrated in Fig. 6 and 7.

Acknowledgements

The author thanks Mario Ishizaki for providing numerical data obtained from the MC simulation in our earlier work. He also thanks Ben Widom for helpful discussions and comments.

This work was supported in part by Grant-in-Aid for Scientific Research from MEXT, Japan.

References

1 R. Lumry, E. Battistel and C. Jolicoeur, *Faraday Symp. Chem. Soc.*, 1982, **17**, 93–108.
2 E. T. Chang, N. A. Gokcen and T. M. Poston, *J. Phys. Chem.*, 1968, **72**, 638.
3 A. Ben-Naim, *Solvation Thermodynamics*, Plenum, New York, 1987.
4 The value is evaluated from the difference in μ^* between water and hydrazine in ref. 1 and μ^* in water in ref. 3.
5 F. Franks, *Water, A Matrix of Life*, Royal Society of Chemistry, Cambridge, 2nd edn, 2000.
6 I. Ohimine and H. Tanaka, *Chem. Rev.*, 1993, **93**, 2545–2566.
7 P. Ball, *Life's matrix: a biography of water*, Farrar, Straus and Giroux, New York, 1st edn, 2000.
8 F. H. Stillinger, *J. Solution Chem.*, 1973, **2**, 141–158.
9 L. R. Pratt and D. Chandler, *J. Chem. Phys.*, 1977, **67**, 3683–3704.
10 W. C. Swope and H. C. Andersen, *J. Chem. Phys.*, 1984, **88**, 6548–6556.
11 K. Watanabe and H. C. Andersen, *J. Phys. Chem.*, 1986, **90**, 795–802.
12 B. Guillot and Y. Guissani, *J. Chem. Phys.*, 1993, **99**, 8075–8094.
13 N. Matubayasi, L. H. Reed and R. M. Levy, *J. Phys. Chem.*, 1994, **98**, 10640–10649.
14 L. R. Pratt, *Annu. Rev. Phys. Chem.*, 2002, **53**, 409–436.
15 B. Widom, P. Bhimalapuram and K. Koga, *Phys. Chem. Chem. Phys.*, 2003, **5**, 3085–3093.
16 S. Rajamani, T. M. Truskett and S. Garde, *Proc. Natl. Acad. Sci. U. S. A*, 2005, **102**, 9475–9480.
17 D. Chandler, *Nature*, 2005, **437**, 640–647.
18 H. S. Ashbaugh and L. R. Pratt, *Rev. Mod. Phys.*, 2006, **78**, 159–178.
19 G. Hummer, S. Garde, A. E. García, M. E. Paulaitis and L. R. Pratt, *J. Phys. Chem. B*, 1998, **102**, 10469–10482.
20 S. Shimizu and H. S. Chan, *J. Chem. Phys.*, 2000, **113**, 4683–4700.
21 K. A. T. Silverstein, A. D. J. Haymet and K. A. Dill, *J. Am. Chem. Soc.*, 1998, **120**, 3166–3175.
22 P. D. Gregorio and B. Widom, *J. Phys. Chem. C*, 2007, **110**, 16060–16069.
23 H. S. Ashbaugh, T. M. Truskett and P. G. Debenedetti, *J. Chem. Phys.*, 2002, **116**, 2907–2921.
24 S. V. Buldyrev, P. Kumar, P. G. Debenedetti, P. J. Rossky and H. E. Stanley, *Proc. Natl. Acad. Sci. U. S. A.*, 2007, **104**, 20177–20182.
25 S. Garde, A. E. García, L. R. Pratt and G. Hummer, *Biophys. Chem.*, 1999, **78**, 21–32.
26 N. Matubayasi, E. Gallicchio and R. M. Levy, *J. Chem. Phys.*, 1998, **109**, 4864–4872.
27 N. M. Cann and G. N. Patey, *J. Chem. Phys.*, 1997, **106**, 8165–8195.
28 D. Ben-Amotz, F. O. Raineri and G. Stell, *J. Phys. Chem. B*, 2005, **109**, 6866–6878.
29 D. Ben-Amotz and B. Widom, *J. Phys. Chem. B*, 2006, **110**, 19839–19849.

30 M. Kinoshita, Y. Harano and R. Akiyama, *J. Chem. Phys.*, 2006, **125**, 244504.
31 M. Ishizaki, H. Tanaka and K. Koga, *Phys. Chem. Chem. Phys.*, 2011, **13**, 2328–2334.
32 J. S. Rowlinson and F. L. Swinton, *Liquids and Liquid Mixtures*, Butterworths, London, 3rd edn, 1982.
33 J. L. F. Abascal and C. Vega, *J. Chem. Phys.*, 2005, **123**, 234505.
34 M. Mezei and D. L. Beveridge, *Ann. N. Y. Acad. Sci.*, 1986, **482**, 1.
35 A contour plot of μ^* for the LJ solvent obtained from the NPT-ensemble simulations is given in Fig. 4 in ref. 31, which is basically the same as Fig. 3a.